Wet front movement and capillary rise testing of a wicking non-woven geotextile component

Gabriele Martins, Md Zahid Hassan, Jamie Bartz & Marolo Alfaro
University of Manitoba, Winnipeg, Manitoba, Canada
Sam Bhat
Titan Environmental Containment Ltd, Île-des-Chênes, Manitoba, Canada
Fernando Portelinha
Department of Civil Engineering – Federal University of São Carlos, São Carlos, São Paulo, Brazil

ABSTRACT
Geosynthetics in pavements provide separation, stabilization, reinforcement and/or drainage functions. A newly developed geogrid composite with wicking non-woven geotextile transports water at zero gradient, utilizing its unique fiber microstructure and proprietary chemical treatment. This study quantifies its unsaturated hydraulic behavior and water transportation abilities through capillary rise and wet front movement tests. Capillary rise tests measured the Water Retention Curve (WRC) under suctions up to 10 kPa. Wet front movement tests were completed in vertical and horizontal directions with the sample submerged in water at one end. Additional horizontal wet front movement tests were performed under applied normal pressure. Results demonstrate the geotextile's ability to transport water over long horizontal distances, even under load, revealing its capability to act as a drainage material in pavement structures. However, further research is needed to assess the geotextile performance in field conditions.

RÉSUMÉ
Les géosynthétiques utilisés dans les chaussées assurent des fonctions de séparation, de stabilisation, de renforcement et/ou de drainage. Un géocomposite à base de géogrille récemment développé, incorporant un géotextile non tissé à effet mèche, transporte à gradient nul, grâce à sa microstructure de fibres unique et à un traitement chimique propriétaire. Cette étude quantifie son comportement hydraulique en conditions non saturées et ses capacités de transport de l'eau à travers des essais de montée capillaire et de déplacement du front d'humidité. Les essais de montée capillaire ont permis de mesurer la courbe de rétention d'eau (CRE) pour des suctions allant jusqu'à 10 kPa. Des essais de déplacement du front humide ont été réalisés verticalement et horizontalement, avec un échantillon immergé dans l'eau à une extrémité. Des essais supplémentaires de déplacement horizontal du front humide ont été effectués sous pression normale appliquée. Les résultats démontrent la capacité du géotextile à transporter l'eau sur de longues distances horizontales, même sous charge, révélant ainsi son potentiel en tant que matériau drainant dans les structures de chaussées. Toutefois, des recherches supplémentaires sont nécessaires pour évaluer les performances du géotextile en conditions de terrain.

1 INTRODUCTION

The design of pavements often incorporates geosynthetics within the road base to perform various functions such as separation, filtration, drainage, reinforcement in the asphalt layer or stabilization in the base layer (Holtz *et al.* 2008, Koerner 2012). Excessive water in the road base, subbase, or subgrade can lead to damage through several mechanisms, including 1) a decrease in the stiffness of the road base due to excess water (AASTHO, 1993); 2) the formation of ice lenses caused by freezing water, which leads to heaving and subsequent weakening of soils upon thawing (Andersland and Ladanyi, 2003); and 3) differential heaving or shrinkage of expansive silty clay subgrades resulting from varying water content (Hamilton, 1980). Consequently, effective water control beneath the pavement surface is expected to enhance pavement performance and reduce distress.

Traditional geotextile fabrics can function as drainage layers and are commonly included in pavement designs as separation between the subgrade and subbase. These geotextiles require saturation and a hydraulic gradient to effectively transport water (Guo et al., 2017). Recent innovations in geosynthetic products have introduced materials that can transport water at zero gradient. One such product consists of geocomposite manufactured with a wicking nonwoven geotextile and geogrid (Jarjour et al., 2024; Liu et al., 2025). This product consists of a high stiffness biaxial geogrid made of polypropylene; heat bonded to a continuous filament nonwoven polyester geotextile with capabilities to transport water against at zero gradient using capillary action. The mechanism to transport water is primarily based on the fiber uniqueness and microstructure of the nonwoven geotextile and further enhanced by chemical treatment.

To understand how a geosynthetic operates under unsaturated conditions, there is a need to study its hydraulic performance under such a state — namely its water retention curve (WRC) and hydraulic conductivity function (K-function) (Zornberg et al. 2010). Other tests like horizontal and vertical wet-front movement can also provide some insights into its wicking abilities. The wet front movements are sometimes stated on technical data sheets for moisture management and wicking geosynthetics.

The WRC characterizes the material's water-holding capacity when it is not in a completely saturated condition, while the K-function characterizes its ability to transmit

water under the same state. Interestingly, the unsaturated K-function depends on the continuity of water paths in the voids, which is governed by the saturation level. As a consequence, the K-function is governed by the WRC and can be predicted from the saturated hydraulic conductivity and the WRC, based on existing models (Mualem 1986; van Genuchten 1980; Fredlund et al. 1994; Fredlund and Rahardjo 1993; Klute 1965).

Studies have investigated the WRC and the differences between wetting and drying paths—commonly referred to as the hysteretic behavior—of non-woven geotextiles (Ho, 2000; Bouazza et al., 2006; Jarjour et al., 2024). The drying paths show higher water content (or degree of saturation) than the wetting paths at the same suction head. Consequently, a reduction in the hydraulic conductivity of the geotextile at low suction pressures (i.e., negative pore-water pressures) is observed (Stormont & Morris, 2000).

However, there are limited publications on the wicking and water transport performance of the wicking nonwoven geotextile component of the geocomposite material in this study. Also, it is unknown if normal pressure on the material affects its ability to laterally transport water due to compression of the material.

The main objective of the research was to quantify the wicking and water transport abilities of the wicking nonwoven geotextile, addressing the existing gap in knowledge regarding its wicking capabilities and the influence of confining pressure on its performance. Specifically, the study aimed to measure the vertical wet-front movement, and horizontal wet-front movement including under normal pressure, as well as the WRC of the wicking geotextile. These measurements sought to provide a comprehensive understanding of the unsaturated behavior of the wicking nonwoven geotextile component of the composite geosynthetic.

2 GEOTEXTILE MATERIALS

Two geosynthetic materials were used in this study including: 1) a wicking nonwoven geotextile-geogrid composite, and 2) a wicking nonwoven geotextile, consistent with material 1 but without the geogrid. A photo of the materials is shown in Figure 1. Table 1 summarizes which tests were completed on each material type. It was not practical to complete all the tests on Material 1 (the composite) because of the geogrid component. Only the vertical wet front movement test was completed on Material 1. All tests were completed on the isolated wicking nonwoven geotextile which was the focus of the study.

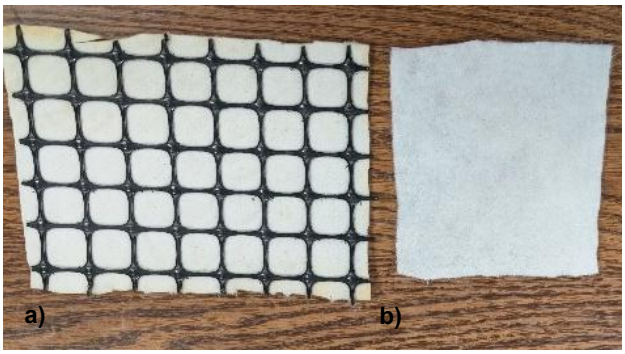

Figure 1. Geosynthetics materials tested: (a) a wicking nonwoven geotextile-geogrid geocomposite; and (b) a wicking nonwoven geotextile.

Table 1. Materials used for each Lab Test

Material	Description	CRT[1]	OE[2]	VWFM[3]	HWFM[4]
1	Wicking nonwoven geotextile-geogrid composite			X	
2	Wicking nonwoven geotextile	X	X	X	X

[1]Capillary Rise Test
[2]Oedometer Test
[3]Vertical Wet Front Movement
[4]Horizontal Wet Front Movement

Table 2 presents additional physical properties for the wicking nonwoven geotextile material, with the Mass per Unit Area (MA) and the Apparent Opening Size (AOS) taken from the manufacturer's specifications and procedure based on ASTM standards D5261 (ASTM 2018) and D 4751 (ASTM 2021), respectively. The thickness (t) is the average back-calculated from 4 saturated samples used to perform the capillary rise test, and the porosity (n) was calculated according to the equation provided in Equation 1 (Bouazza et al. 2006).

Table 2. Geotextiles basic characteristics

Material	MA[1] (g/m^2)	t (mm)	n[2]	AOS (mm)[3]
2	235	3.66	0.95	0.194

[1]mass per unit area
[2]porosity
[3]Apparent Opening Size

$$n = 1 - \frac{M_A}{t\rho_f} \quad [1]$$

Where M_A is the mass per unit area, ρ_f is the fiber density, and t is the specimen thickness.

3 EXPERIMENTAL PROGRAM

3.1 Capillary Rise Test

A capillary rise test shown in Figure 2 was employed to measure the water characteristic curve for Material 2 under wetting and drying conditions. Numerous studies have employed the capillary rise test to measure the water characteristic curve of geosynthetics (Park and Fleming 2004, Krisdani *et al.* 2008, Lin *et al.* 2023, Jarjour *et al.* 2024). The procedure for determining the drying and wetting curves is outlined below. Strips of known dimensions (0.1 x 1.0 m) were cut for each test. In the drying condition, the strips were initially saturated. In the wetting condition, the strips began in a dry state. The geotextile was then suspended with its lower end submerged in water, and a plastic protective covering was applied around the textile to minimize the effect of evaporation. Two samples were tested for both the wetting and drying conditions.

The sample was allowed to reach equilibrium over a period of approximately 10 days. Subsequently, the geotextile was cut into thin strips, and the height to the midpoint of each strip above the water table was measured to obtain the volumetric water content along the strip height. The suction for each strip was calculated based on the measured height above the water table according to Equation 2.

$$\psi = \rho_w g h \quad [2]$$

Where ψ is the matric suction (Pa), h is the elevation of the specimen above the water table (m), ρ_w is the density of water (Kg/m^3), and g is the gravitational acceleration (m/s^2).

To construct the water characteristic curve, the suction needs to be plotted against the saturation (S) or volumetric water content. The saturation (S) of each strip was calculated according to Equation 3. The volumetric water content (θ) was calculated from Equation 4.

$$S = \frac{w\, M_A}{t\, n\, \rho_w} \quad [3]$$

$$\theta = S\, n \quad [4]$$

Where w is the water content, M_A is the mass per unit area, t is the specimen thickness, n is the porosity, ρ_w is the density of water, and θ is the volumetric water content.

Figure 2. Capillary rise test equipment

At the air entry value (AEV, ψ_a) – which represents the suction at which drainage begins – air enters through the largest external pore. This value can be determined graphically, as shown in Figure 3. From this point onward, the water content decreases rapidly with increasing suction until the residual volumetric water content is reached (as shown in Figure 3). Beyond this point, any further removal of water from the geotextile or other porous materials would require vapor migration. The wetting curve is the inverse of the drying curve, where moisture content is plotted against matrix suction as it increases. Similar to the drying curve, a wetting entry value can be determined graphically, indicating the suction level at which water begins to flow through the porous material.

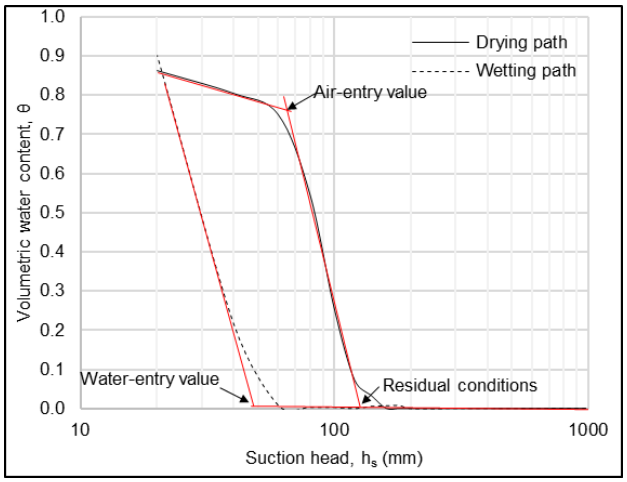

Figure 3. Typical water-retention variation on drying and wetting paths.

3.2 Vertical Wet front movement test

A vertical wet front movement test was performed to quantify the wicking ability of the wicking nonwoven geotextile. During the tests, the temperature was recorded at 21.5 °C for the geocomposite and 21.7°C for the wicking geotextile and relative humidity was recorded at 24% for both materials. The test consisted of hanging a dry sample (0.3 m wide by 0.3 m tall) and submersing the bottom into water. This is similar to the test set up shown in Figure 2 with different sample dimensions. The wet front was visually documented and recorded against time until the wet front reached a maximum height. Dye was used to assist with the visual observation of the vertical wet front. The test was performed on the two materials including the wicking geotextile-geogrid composite and a sample of just the wicking nonwoven geotextile.

3.3 Horizontal Wet front movement test

A modified horizontal wet front movement test was performed with the geotextile specimen placed on a level wooden table. This was done to allow for compressing the fabric to study the effect of surcharge pressure on its horizontal wicking abilities. In field application, the geosynthetic will similarly be subject to normal pressure compressing the fabric. It should be noted that the normal horizontal wet front movement results reported on data sheets is based on the geosynthetic being elevated and not resting on a surface. A geotextile specimen measuring 0.3 m in width and 1.0 m in length was placed on the horizontal wooden table as shown in Figure 4, with both ends securely fixed to maintain a level position. The water table within the reservoir was kept at the same elevation as the geotextile specimen to ensure zero hydraulic gradient. Three types of tests were conducted: the first without any applied load, the second with an acrylic sheet (t = 9 mm and ρ = 1.18 g/cm^3) placed over the specimen, and the third with a 8.8 kPa of applied surcharge. The surcharge load was applied by the placement of steel plates on top of the acrylic. Gaps were left between steel plates to allow observation of movement of the wet front. The average normal stress was calculated by dividing the total force from the weight by the total area of the geosynthetic. There may be some variation in normal pressure due to the gaps in the weights, but the acrylic sheet above the geotextile was placed to distribute the load for more even pressure distribution. Figures 5 and 6 show the test setup with and without the surcharge load. Movement of the wet front was recorded over time, and a yellow dye was introduced to enhance the visualization of water movement. The test continued until the water fully traversed the specimen.


Figure 4. Table for modified horizontal wet front movement test


Figure 5. Horizontal wet front movement test without load

Figure 6. Horizontal wet front movement test with load

3.4 Determination of geotextile thickness under normal pressure

An oedometer test apparatus was used to measure the thickness of the geotextile when subjected to various normal pressures. The test was conducted to correlate the thickness change due to applied normal pressure with the results from the horizontal wet front movement test, assessing how pressure affects water transport within the material. The applied normal pressures were approximately 1 kPa, 2 kPa, 5.4 kPa, 10 kPa, 15 kPa, and 20 kPa.

4 RESULTS AND DISCUSSIONS

4.1 Capillary rise test

Figure 7 presents the Water Retention Curve (WRC) for the tested geotextile samples, illustrating the drying and wetting path behavior of the wicking geotextile. The test was performed in duplicate for the geotextile samples. A pronounced hysteresis effect was observed in the wicking geotextile, with the drying curve consistently retaining more water than the wetting curve. Two data points for the drying curve path 2 (marked with a black circle) appear to be erroneous as they do not reflect the anticipated shape of a WRC. A potential source of this error could have been from cutting and handling the sample. Water could have been expelled from the cut sample in this process, lowering the water content.

The AEV is approximately 0.7 kPa and the water entry value (WEV, ψ_w) is approximately 0.5 kPa based on the WRC in Figure 7. It should be noted that Jarjour et al. (2024) reported an AEV of 1.4 kPa performing the capillary rise test on the same material. One potential cause of this discrepancy could be due to differences in humidity for the test conditions. Relative humidity of the room was recorded as approximately 24% during the testing. Evaporation is expected from the samples at this humidity. The samples were protected with plastic to prevent evaporation, however, Park and Fleming (2004) suggested that some evaporation is expected with the hanging test. As an alternative to the hanging capillary rise test, they suggest performing a pressure plate test to prevent evaporation and demonstrated that the WRC differs when using a pressure plate test apparatus.

Iryo and Rowe (2003) reviewed published literature and summarized WRC results from 14 nonwoven geotextiles. They reported that most geotextiles had an AEV between 0.4 and 1.2 kPa, and two materials had an AEV exceeding 1.2 kPa. Their review summarized that most samples had a WEV between 0 and 0.8 kPa. The AEV and WEV of the wicking nonwoven geotextile in this study were within this normal range for nonwoven geotextiles.

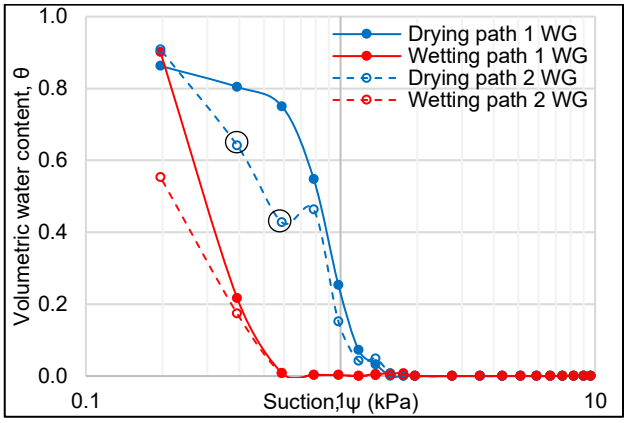

Figure 7. Hanging test water-characteristic curves for the wicking nonwoven geotextile

4.2 Vertical Wet Front Movement Test

The results obtained from the wicking nonwoven geotextile and for the composite material with the geogrid are shown in Figure 8. Figure 8a shows that the wet front stabilized before 110 minutes, indicating the cessation of flow for both materials. A notable difference emerged by 110 minutes, at which point the composite exhibited a greater wet front advancement (0.07 m) compared to the geotextile alone (0.05 m). It is not clear whether this discrepancy is due to variability in the nonwoven geotextile, the heat bonding process, or some other factor.

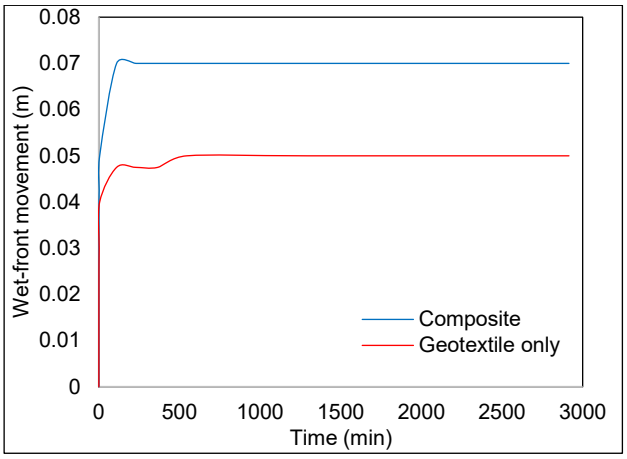

Figure 8. Vertical wet front movement curves

4.3 Horizontal Wet Front Movement Test

The measurements from wet-front migration in the wicking nonwoven geotextile in the horizontal direction for unloaded and loaded states (acrylic and weight tests) were conducted using a modified procedure based on ASTM C 1559 (ASTM, 2021). The results are presented in Figure 9. The results have been compared to another test, which was run by SGI Testing Services, that was performed with the test suspended in the air. The test by SGI measured a horizontal wet front movement of 2.3 m at 983 minutes. A wet front movement for the same duration (983 minutes) could not be established for the modified tests on the table as the wet front exceeded the 3 m length of the table before this time. Figure 9a depicts that the horizontal wet front reached the end of the table fastest for the loaded specimen, followed by the specimen placed under the acrylic layer, then the specimen resting on the table and exposed to the air. Figure 9b shows rapid initial wet-front progression across all conditions, followed by a gradual decrease in velocity for all three tests reaching a minimum value of approximately 0.43, 0.54 and 0.60 m/h at the end of test for the unloaded, acrylic, and loaded conditions respectively. The wet front velocity was considerably greater when resting on the table after about 100 minutes compared to the elevated sample testing by SGI. Figure 9c shows the decrease in wet-front velocity with the distance for all cases, illustrating the difficulty of transport as the material gets further from the source of water.

The three conditions for the modified wet front movement test had relatively similar results. The SGI test (black dashed line) for an elevated sample exhibited a wet-front pattern similar to the unloaded condition until the wet-front reach approximately 2 m, suggesting that both configurations facilitated similar water transport mechanisms. It was noted during testing by SGI that water dripped from the samples. It is believed that the modified tests on the table maintained higher velocities after the wet front reached 2 because water could not drip out of the sample. The modified test set up with the sample resting on the table may better reflect field conditions if the geotextile is placed over a low permeability subgrade. Overall, the results underscore the influence of external conditions on horizontal water transport in geotextiles.

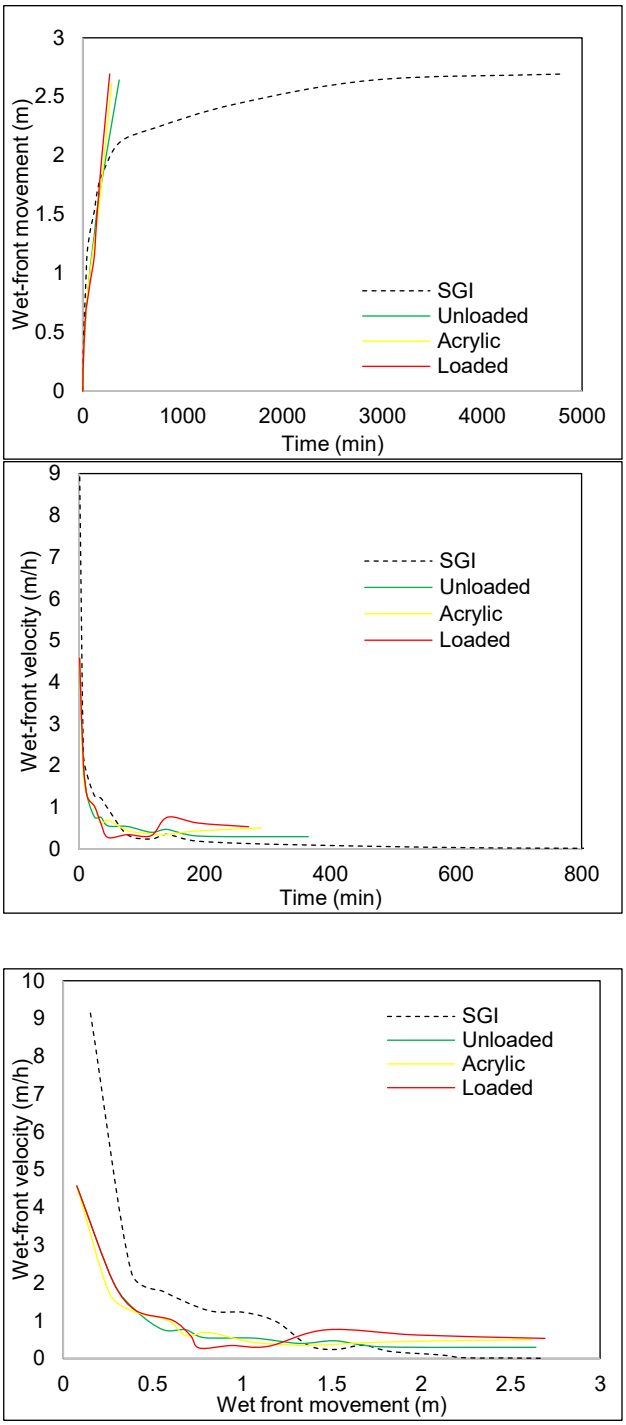

Figure 9. Wet front movement plot along geotextile in the horizontal direction (ASTM C 1559 Modified): (a) time versus wet-front movement; (b) time versus wet-front velocity; (c) wet-front movement versus wet-front velocity

These trends are consistent with the observations reported by Sicha, Chen, and Zornberg (2023), conducted experiments involving a 0.2-m-wide by 1-m-long geotextile with enhanced drainage characteristics to examine spontaneous horizontal flow that is completely due to capillary forces. Their study documented a decline in flow after approximately 100 minutes, along with a marked deceleration in wetting front velocity. They also noted a sharp initial reduction in velocity within the first 0.1 to 0.2 m of flow, followed by a gradual decrease. Such behavior aligns with the deceleration trends observed in Figure 9c. Furthermore, they emphasized the variability in experimental results under different laboratory conditions, which supports the need to interpret horizontal flow tests with caution. Altogether, both sets of results reinforce the complex interaction between material properties, capillarity, and boundary conditions in governing unsaturated flow behavior in geotextiles.

4.4 Thickness *versus* normal pressure

Figure 10 illustrates the relation between thickness and normal pressure. Seven different pressure levels were considered: 0, 1, 2, 5.4, 10, 15, and 20 kPa. The 0 kPa value was back-calculated using the saturation equation, while the remaining values were obtained through oedometer testing.

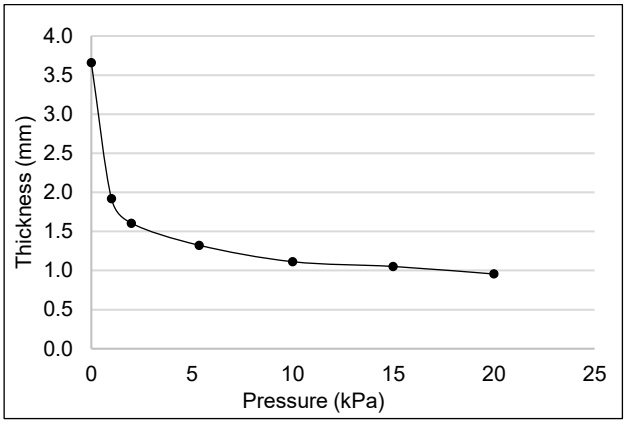

Figure 10. Thickness as a function of the normal pressure applied to the nonwoven geotextile

The observed compression behavior implies that as pressure increases, the stiffness of the materials also increases, making additional thickness reduction progressively smaller. This trend may have implications for their ability to retain void space and influence fluid movement under load.

During the horizontal wet front movement test with weights, the normal pressure was approximately 8.8 kPa. The horizontal wet front movement tests indicated that the geotextile was effective at horizontally moving water under zero gradient for each test condition, however, additional normal stress would further compress the fabric as indicated in Figure 10. Horizontal wet front movement tests were not conducted at these higher stresses where the geotextile is less thick.

5 CONCLUSIONS

The series of laboratory tests were performed to evaluate the wicking and water transporting function of a wicking nonwoven polyester geotextile and geogrid composite. For practical reasons, several tests were conducted on only the geotextile component. The following conclusions are drawn from this study:

- The modified wet front movement test with the sample on a surface enhanced the lateral movement of water after the horizontal wet front reached approximately 2 m compared to a wet front movement test with a sample elevated. The wet front reached the end of the table (3.0 m) in approximately 270 to 370 minutes for the various test conditions. This exceeds the 2.301 m after 983 minutes reported on the data sheet. It is believed that this enhancement is due to the test set up preventing water from leaving the system compared to the elevated sample where water can drip out of the sample and may be more representative of field conditions if the geotextile is installed over a low permeability subgrade.
- The nonwoven geotextile compresses with normal pressure. There was not a significant difference in horizontal wet front movement in the modified test with placement of weights on the sample which decreased sample thickness.
- The vertical wet front reached 0.05 m for the wicking nonwoven geotextile and 0.07 m or the composite material. It is not clear whether this discrepancy is due to variability in the nonwoven geotextile, the heat bonding process, or some other factor.
- The capillary rise test indicated an air entry value of approximately 0.7 kPa and a water entry value of approximately 0.5 kPa. These values fall within the reported range for other nonwoven geotextiles. The air entry value measured in this study differs from results on the same product reported by others which could be attributed to differences in test condition humidity and evaporation.

Additional testing is required to quantify the unsaturated and wicking behaviour of this composite material. Pressure plate testing could provide a more reliable water retention curve to overcome limitations regarding evaporation from a hanging capillary rise test. Laboratory and field tests are required to quantify the ability of the composite geosynthetic to transport water when in contact with soil.

6 REFERENCES

ASTM. 2021. Standard test method for determining wicking of fibrous glass blanket insulation (aircraft type). *ASTM C1559 – 15 (Reapproved 2021).* West Conshohocken, PA: ASTM.

ASTM. 2018. Standard test method for measuring mass per unit area of geotextiles. *ASTM D5261 – 10 (Reapproved 2018).* West Conshohocken, PA: ASTM.

American Association of State Highway and Transportation Officials. (1993). *AASHTO guide for design of pavement structures*. Washington, DC: AASHTO.

Andersland, O. B., & Ladanyi, B. (2003). *Frozen ground engineering* (2nd ed.). John Wiley & Sons.

ASTM. 2021. Standard test methods for determining apparent opening size of a geotextile. *ASTM D4751 – 21a.* West Conshohocken, PA: ASTM.

Bouazza, A., Freund, M., & Nahlawi, H. (2006). Water retention of nonwoven polyester geotextiles. *Polymer Testing*, 25(8), 1038–1043.

Guo, J., Wang, F., Zhang, X., & Han, J. (2017). Quantifying water removal rate of a wicking geotextile under controlled temperature and relative humidity. *Geotextiles and Geomembranes*, 45(5), 302-312. https://doi.org/10.1016/j.geotexmem.2017.04.003

Holtz, R. D., Christopher, B. R., & Berg, R. R. (2008). *Geosynthetic design and construction guidelines* (FHWA NHI-07-092). Federal Highway Administration.

Iryo and Rowe (2003) On the behaviour of unsaturated nonwoven geotextiles. *Geotextiles and Geomembranes*, 21 (6), 381 – 404.

Jarjour, J., Meguid, M., & Bhat, S. (2024). Water retention characterization of non-woven geotextiles: An application for wicking materials. In *Proceedings of the 5th Pan-American Conference on Geosynthetics*. Toronto, Canada.

Koerner, R. M. (2012). *Designing with geosynthetics* (6th ed.). Pearson.

Lin, C., Guo, Y., Zhang, X., & Galinmoghadam, J. (2023). Reexamination of traditional testing techniques for determining WRCs of woven geotextiles in full suction range. *Geotextiles and Geomembranes*, 51(5), 1–16. https://doi.org/10.1016/j.geotexmem.2023.04.007

Liu M, Liu J, Bhat S, Gao Y., Lin C. (2025) Model tests on wicking geosynthetic composite reinforced bases over weak subgrade. *Geotextiles and Geomembranes* 53:938–949. https://doi.org/10.1016/j.geotexmem.2025.03.006

Park, K. D., & Fleming, I. R. (2004). Determination of the unsaturated properties of a nonwoven polypropylene geotextile for use as part of a geocomposite capillary barrier. In *Proceedings of the 57th Canadian Geotechnical Conference* (Session 5E, pp. 36–43). Quebec, Canada.

Sicha, G., Chen, K., & Zornberg, J. (2023). Quantification of suction-driven flow of enhanced lateral drainage in geotextiles. *Geo-Congress 2023*, ASCE. https://doi.org/10.1061/9780784484734.037

Stomont. J.C. and Moms. C.E.. 2000. "Characterization of Unsaturated Nonwoven Geotextiles". Advances in Urzsaturated Georechnics, Shackelford. CD., Houston, S.L. and Chang, N.Y.. Editors, Geotechnical Special Publication No. 99. *Proceedings of sessions of Geo-Denver 2000 sponsored by the Geo-Institute of the ASCE*. Denver, Colorado. USA. August 2000, pp. 529-542.

7 ACKNOWLEDGEMENTS

This work was supported by Emerging Leaders in the Americas Program (ELAP). We acknowledge the support of the Natural Sciences and Engineering Research Council of Canada (NSERC) [ALLRP 585874 – 23].